where x is the coordinate in the streamwise direction, y is the coordinate in the direction normal to the channel wall, $y = 0$ designates the centerline of the channel, β_n values are the positive roots of $\beta = \tan\beta (0 < \beta_1 < \beta_2 < \cdots)$, and Re is based on the characteristic length and the average axial velocity. This velocity field represents a flow that starts impulsively at $t = 0$, and at steady state coincides with two-dimensional Poiseuille flow.

There is no inherent upper limit to the Reynolds number that can be computed with the CIP-ACE method. We examined a representative case, namely, $Re = 100$. The calculation was carried out for a rectangular region bounded by $0 \leq x \leq 6$ and $0 \leq y \leq 1$, which was discretized into a 61×11 uniform grid. The calculation used a time step of $\Delta t = 0.01$, an artificial compressibility constant of $\beta = 2000$, and a pseudotime step of $\Delta\tau = 100$.

At each time step, Eq. (5) was solved until a steady-state solution was achieved in pseudotime. During the initial transient stage (near $t = 0$), five to six pressure subiterations were required for calculating the pressure at each time step, but decreased with time to three subiterations. The maximum divergence of velocity was less than 10^{-6} at each time step. Figure 1 shows a comparison between the calculated and the exact solution. The axial velocity profiles are shown at the channel outlet for two different time points. The calculated results are fairly close to the exact solutions except for those near the channel wall and for the initial transient stage ($t = 0.4$, for example). These differences, however, diminish with time. Moreover, agreement can be improved by using a finer grid.

Conclusions

We presented a procedure for computing time-accurate solutions to the incompressible N-S equations. The procedure, which we designated the CIP-ACE method, uses 1) an artificial compressibility approach to transform the equations into a hyperbolic system, 2) a fractional-step-like approach, and 3) cubic-polynomial interpolation to upwind difference the N-S equations. A formal procedure based on a fractional-step-like approach is used to split the momentum equation into a nonadvection equation and an advection equation. The nonadvection equation is solved using a steady-state solution of the diffusion equation for pressure in pseudotime, whereas cubic-polynomial interpolation is used to solve the advection equation. To validate this CIP-ACE method, we solved two sample incompressible flow problems with known exact solutions. For each problem, the method showed rapid convergence to a numerical solution that is reasonably compatible with the exact solution. The CIP-ACE method can be extended in a straightforward manner to solve the three-dimensional, incompressible N-S equations in generalized coordinates, making it an attractive alternative to more established numerical methods.

References

[1]Yabe, T., and Wang, P. Y., "Unified Numerical Procedure for Compressible and Incompressible Fluid," *Journal of the Physical Society of Japan*, Vol. 60, No. 7, 1991, pp. 2105–2108.

[2]Yabe, T., "A Universal Cubic Interpolation Solver for Compressible and Incompressible Fluids," *Shock Waves*, Vol. 1, No. 2, 1991, pp. 187–195.

[3]Yabe, T., and Aoki, T., "A Universal Solver for Hyperbolic Equations by Cubic-Polynomial Interpolation I. One-Dimensional Solver," *Computer Physics Communications*, Vol. 66, No. 3, 1991, pp. 219–232.

[4]Yabe, T., Ishikawa, T., and Wang, P. Y., "A Universal Solver for Hyperbolic Equations by Cubic-Polynomial Interpolation II. Two- and Three-Dimensional Solvers," *Computer Physics Communications*, Vol. 66, No. 3, 1991, pp. 233–242.

[5]Rogers, S. E., and Kwak, D., "Upwind Differencing Scheme for the Time-Accurate Incompressible Navier-Stokes Equations," *AIAA Journal*, Vol. 28, No. 2, 1990, pp. 253–262.

[6]Golub, G. H., and Van Loan, C. F., *Matrix Computations*, 2nd ed., Johns Hopkins Univ. Press, Baltimore, MD, 1990.

[7]Harlow, F. H., and Welch, J. E., "Numerical Calculation of Time-Dependent Viscous Incompressible Flow with Free Surface," *Physics of Fluids*, Vol. 8, No. 12, 1965, pp. 2182–2189.

[8]Takemitsu, N., "Finite Difference Method to Solve Incompressible Fluid Flow," *Journal of Computational Physics*, Vol. 61, No. 3, 1985, 499–518.

Assessment of Pressure-Strain Models in Predicting Compressible, Turbulent Ramp Flows

R. Abid*
High Technology Corporation, Hampton, Virginia 23666
Thomas B. Gatski†
NASA Langley Research Center, Hampton, Virginia 23681
and
Joseph H. Morrison‡
Analytical Services & Materials, Inc., Hampton, Virginia 23666

Introduction

THE purpose of this Note is to evaluate the performance of three pressure-strain correlation models (linear, quadratic, and cubic in the Reynolds stress anisotropy tensor) in the prediction of a compression ramp flow of 16 deg. Although compression ramps represent only one class of nonequilibrium flow, they have important practical application in the design of high-speed vehicles and propulsion systems. Variations in the ramp angle can lead to flows that range from an attached two-dimensional flow to a fully separated, three-dimensional unsteady flow. Clearly, the latter limit is outside the scope of the present study; however, for a ramp angle of 16 deg only incipient separation is observed experimentally at the ramp and flat-plate juncture, and experimental results[1] show that the flow is two dimensional. Thus, the flow turbulence along the ramp is initially induced by the shock-boundary-layer interaction at the flat plate and ramp juncture, and the flow can serve as a test of pressure-strain correlation models to predict an important type of compressible flowfield.

In any closure validation study, the first step is clearly the isolation of each particular correlation closure; in the present study, the focus will be on the pressure-strain correlation. In the solution of compressible flowfields, variable-density extensions to the incompressible forms of these pressure-strain models have been generally used. Thus, a variety of incompressible pressure-strain models can be tested to assess their applicability to compressible flow predictions.

The present study utilizes wall functions so that the effects of the pressure-strain models can be isolated. Care must be exercised in the implementation of the wall functions to insure a smooth functional behavior of the dependent variables throughout the inner part of the boundary layer. Equilibrium conditions consistent with the existence of a logarithmic region are assumed; these must also be consistent with the compressible models introduced for the various correlations. Unfortunately, not all turbulence models satisfy the Van Driest law of the wall when applied to compressible flows because they yield values for the von Kármán constant κ that differ from the accepted value of 0.41. In this regard, Wilcox[2] and Huang et al.[3] have examined the effect on the value of κ for both the K-ω and K-ε models with the compressibility corrections of Zeman[4] and Sarkar et al.[5] and found that these models cause a deviation of the log-law slope. For this reason, these explicit compressibility corrections for the dissipation rate and pressure dilatation are omitted, and a single-layer wall-function formulation is used in conjunction with variable-density extensions of the incompressible pressure-strain correlations.

Received June 17, 1993; revision received Oct. 5, 1994; accepted for publication Oct. 11, 1994.

*Senior Scientist, 28 Research Drive. Member AIAA.
†Senior Research Scientist, MS 128.
‡Senior Research Scientist. Member AIAA.

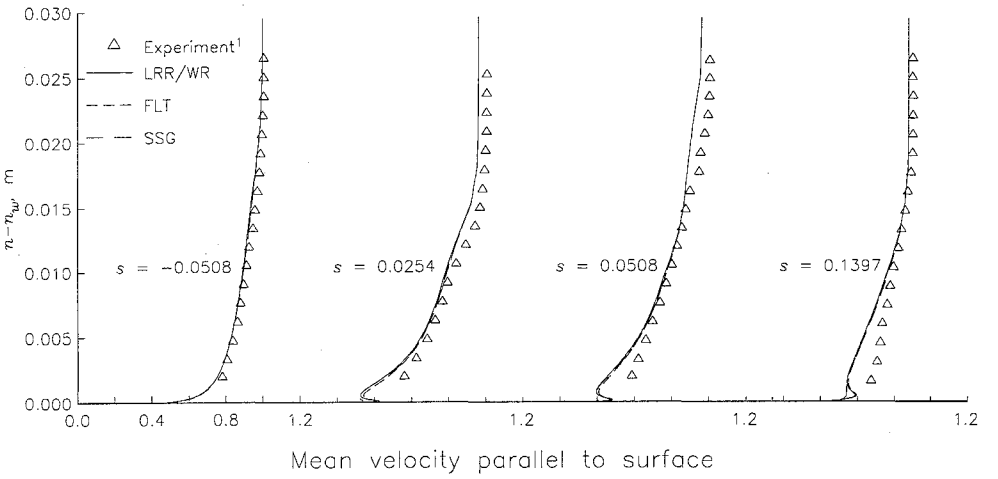

Fig. 1 Comparison of streamwise mean velocity with experimental results at streamwise locations of $s = -0.0508, 0.0254, 0.0508$, and 0.1397 m.

Formulation for Compressible, Turbulent Flow

The formulation of the mean conservation and Reynolds stress transport equations has been given previously[6] in a study of near-wall turbulent closure models. In the present study, the same formulations are used, but the near-wall pressure-strain correlation model is replaced by a high-Reynolds-number model that is not valid in the near-wall region. Three different high-Reynolds-number models are tested in conjunction with a suitable wall-function distribution in the near-wall region.

Because the focus of this work is to study the performance of a variety of pressure-strain models in predicting the flow over a compression ramp, three representative models will be analyzed: the model of Launder, Reece, and Rodi with wall reflection[7] (LRR/WR); the model of Speziale, Sarkar, and Gatski[8] (SSG); and the model of Fu, Launder, and Tselepidakis[9] (FLT). These models are either linear (LRR/WR), quadratic (SSG), or cubic (FLT) in the anisotropy tensor $b_{ij} = (\tau_{ij} - \frac{2}{3}K\delta_{ij})/2K$ (where τ_{ij} is the Reynolds stress tensor and K is the turbulent kinetic energy) and are assumed to be only functions of the anisotropy $\boldsymbol{b}$ and the symmetric and antisymmetric parts of the mean velocity gradient, $\tilde{S}_{ij} = (\tilde{u}_{i,j} + \tilde{u}_{j,i})/2$ and $\tilde{W}_{ij} = (\tilde{u}_{i,j} - \tilde{u}_{j,i})/2$, respectively.

Coupled with the Reynolds stress transport equations, which use each of the aforementioned pressure-strain models, is a dissipation rate equation. The high-Reynolds-number form[6] of this equation contains the three unknown coefficients $C_{\varepsilon 1}$, $C_{\varepsilon 2}$, and C_ε, which are associated with the production, destruction, and diffusion terms in the equation, respectively. The values for the $C_{\varepsilon 1}$ and $C_{\varepsilon 2}$ coefficients associated with the three pressure-strain models are $C_{\varepsilon 1} = 1.44$ and $C_{\varepsilon 2} = 1.90$ for the LRR/WR model, $C_{\varepsilon 1} = 1.44$ and $C_{\varepsilon 2} = 1.83$ for the SSG model, and $C_{\varepsilon 1} = 1.45$, and $C_{\varepsilon 2} = 1.90$ for the FLT model. In the LRR/WR and SSG models, the dissipation rate ε_{ij} is modeled through the usual isotropic assumption $\varepsilon_{ij} = \frac{2}{3}\varepsilon\delta_{ij}$; in the FLT model, the tensor dissipation rate explicitly accounts for anisotropic effects.[9] The choice of diffusion coefficient C_ε has been the subject of a recent study.[10] To insure the correct log-layer slope, C_ε needs to be chosen consistent with the equilibrium stress anisotropy levels in the log-layer given by each model. Such an analysis yields the $C_\varepsilon = 0.26$, 0.18, and 0.19 for the LRR/WR, SSG, and FLT, respectively. The values, although strictly applicable to the incompressible regime, can be applied to this compressible case because of the small influence of compressibility. As mentioned earlier, the compressible formulation may yield values of the log-law slope that differ from the usual $1/\kappa$ value. Based on the estimates given by Wilcox[2] for the freestream Mach number under consideration here, the deviation from the usual $1/\kappa$ value is only about 0.5%. Since the SSG pressure-strain model has not been coupled and calibrated with any specific turbulent diffusion model, it is necessary, for a consistent study, to use the same turbulent diffusion model in conjunction with all three pressure-strain correlation models. The turbulent diffusion model used here is the Hanjalic and Launder model as given in Launder et al.[7] using the closure coefficient of 0.11.

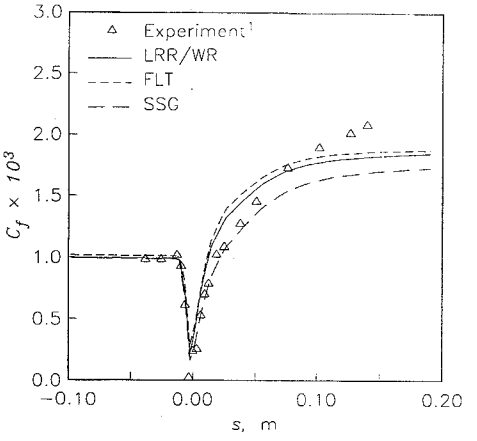

Fig. 2 Normalized skin-friction variation along flat-plate and ramp surface.

The procedure for the wall function implementation[11] utilizes the usual log-law and equilibrium assumptions common for flat-plate boundary-layer flows. Nevertheless, these wall functions are applied throughout the flow domain, even in the vicinity of the ramp and flat-plate juncture. Because the separation is only incipient in this flow, the wall-function procedure should still be applicable.

Results and Discussion

The calculation procedure follows that outlined in Morrison et al.[6] The flowfield is computed from the freestream to a point in the fully turbulent regime at which the profile distributions closely approximate experimental conditions. To match the inflow profiles to the experimental results, a location is selected at which the boundary-layer thickness, the displacement thickness, and the momentum thickness are all within 15% of their experimental values. The distance normal to the flat-plate surface is designated as y; along the ramp, the normal distance is designated as n. In all figures, the mean streamwise velocity $\tilde{u}$ and the Reynolds stress components τ_{ij} are scaled by U_∞, T_∞, and U_∞^2, respectively; however, the distances normal to the surface (either y or n) are left dimensional. This mixed convention is used so that the computational results compare directly with the experimental results. The locations of the four measuring stations downstream of the inflow plane, where the actual results are compared with the computed results, can be described relative to the boundary-layer thickness of the incoming mean velocity profile, which is 0.0254 m.[12] In the present coordinate system, the origin is located at the flat-plate and ramp juncture, so that upstream of the ramp along the flat plate the values of s are negative. With this measure for the 16 deg ramp, the first station is located at $s = -0.0508$ m, and the downstream stations are $s = 0.0254$, 0.0508, and 0.1397 m. A 81 × 51 mesh is used with a variable grid spacing in the normal direction. The first solution point is chosen so that it is located

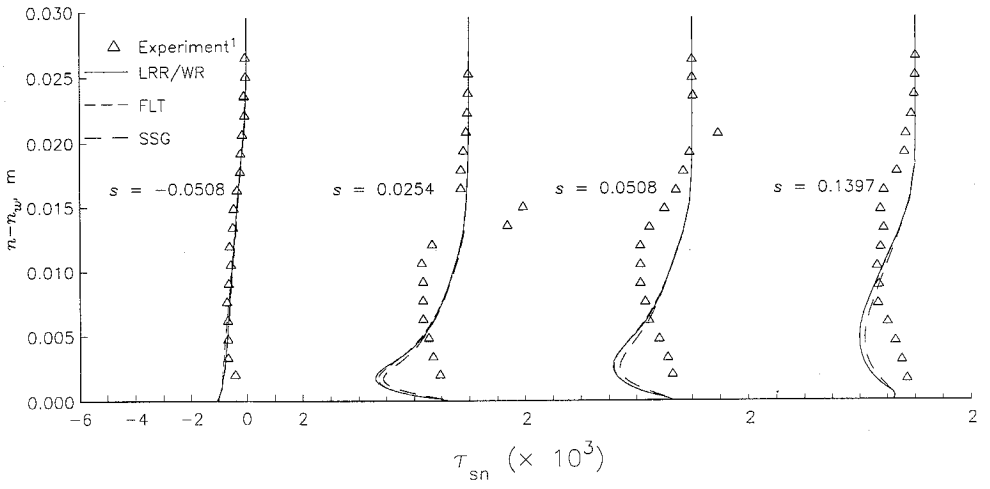

Fig. 3 Comparison of τ_{sn} with experimental results at streamwise locations of $s = -0.0508, 0.0254, 0.0508$, and 0.1397 m.

in the logarithmic region ($30 < y_f^+ < 70$) for all streamwise locations. Previous grid-resolution studies on these configurations[6] have shown this level of discretization to yield essentially grid-independent results.

A comparison of the computed streamwise mean velocity with that of the experimental results at the four streamwise stations is shown in Fig. 1. As the figure shows, the results from all three pressure-strain models are very similar, which indicates that given a consistent inflow profile satisfying the log-law, the streamwise velocity appears unaffected by the particular choice of pressure-strain model. In all three models a velocity defect with experiment exists downstream along the ramp. The deterioration in agreement is most evident in the lower regions near the wall.

Figure 2 is a plot of the variation of skin friction along the flat-plate and ramp surfaces. Both the LRR/WR and FLT models respond similarly along the flat plate and ramp start, especially when the slightly higher FLT flat-plate skin-friction value is taken into account. The SSG model also responds correctly along the flat plate and ramp start but shows a smaller minimum c_f value at the juncture that is more consistent with the experiment. Along the ramp, all three models fail to reach the experimental peak value. The LRR/WR and FLT models response is too rapid to the imposition of the ramp, whereas the SSG model response is more in line with the experiment but relaxes back too quickly toward the flat plate value.

The more rapid relaxation of the skin friction along the ramp for the SSG model relative to the other models suggests a more rapid relaxation for the shear stress in this region as well. Comparisons between the computed Reynolds shear stress and the measured data are shown in Fig. 3. For all four stations, the models yield the same qualitative results; however, the SSG model result, as anticipated, is smaller in magnitude than either the LRR/WR or FLT models. The location of the peak stress levels at the three stations downstream of the ramp juncture are predicted too close to the wall, and the peak stress levels are overpredicted for all three models.

The ability of all three models to predict both the response of the turbulence through the shock and the relaxation of the turbulence downstream of the ramp juncture is best shown by comparing the computational results with experimental data[13] along a streamline in the flow. Figure 4 shows the evolution of the τ_{ss} (normalized by its inflow value τ_{ss0}) correlation along a streamline that originates at the point $y/\delta_0 = 0.2$ at the inflow plane on the flat plate. This location corresponds to a y^+ value of about 2200 at the inflow and is well away from the wall-function interface. Thus, the results should only reflect the effects of the high-Reynolds-number pressure-strain correlation models. None of the models are capable of predicting the rapid response of the turbulence through the shock. Compressibility effects exhibited through the dilatation dissipation or pressure dilatation may need to be included to properly account for the effects of the shock. In addition, the pressure-strain correlation models themselves may not be capable of handling such rapid mean flow distortions. Farther downstream, the computational

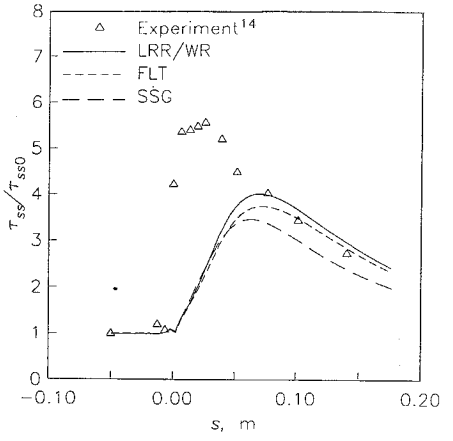

Fig. 4 Evolution of normalized τ_{ss} along streamline that originates at $y/\delta_0 = 0.2$.

results slowly relax back to the equilibrium values, although experimental data are not available sufficiently far downstream to show the ultimate agreement. Note that even at a distance of six boundary-layer thicknesses downstream, the turbulence has not yet relaxed to its preshock level.

In summary, the objective of this study was to isolate the effect of the pressure-strain correlation term in the prediction of a compression ramp flow where shock-boundary-layer interaction had a significant effect on turbulence amplification. Variable density extensions of three incompressible pressure-strain models were tested in a consistent manner to assess their performance. All models used the same wall functions and turbulent diffusion models and displayed the correct log-law behavior along the flat plate before the ramp start. The study showed that all of the models had difficulty in predicting the rapid response of the turbulence to the presence of the shock. In addition, all of the models showed an improper redistribution among the stress components; an overprediction of the peak shear stress component (Fig. 3) and an underprediction of the normal stress component (Fig. 4). These results imply that the variable-density extensions of incompressible pressure-strain correlation models are insufficient in themselves to properly account for the effects of turbulence amplification through a shock. Improved accounting of anisotropic stress effects and improved accounting of turbulence levels necessarily need to be included in such shock-boundary-layer flows. Only recently have efforts been made to assess the effect of the variable-density assumption.[14] At least for the case of homogeneous shear flow, the variable-density extensions were unable to properly account for the behavior of the Reynolds stress anisotropies. Whether this deficiency, or some other effect such as a poorly formulated (an)isotropic dissipation rate equation is the cause of the problem will require further study.

Acknowledgments

This research was supported by the NASA Langley Research Center under Contract NAS1-19299 with High Technology Corporation and under Contract NAS1-19320 with Analytical Services and Materials, Inc.

References

[1]Settles, G. S., and Dodson, L. J., "Hypersonic Shock/Boundary-Layer Interaction Database," NASA CR 177577, April 1991.

[2]Wilcox, D. C., "Turbulence Modeling for CFD," DCW Industries, Inc., La Cañada, CA, 1993.

[3]Huang, P. G., Bradshaw, P., and Coakley, T. J., "Turbulence Models for Compressible Boundary Layers," *AIAA Journal*, Vol. 32, No. 4, 1992.

[4]Zeman, O., "Dilatation Dissipation: The Concept and Application in Modeling Compressible Mixing Layers," *Physics of Fluids A*, Vol. 2, No. 2, 1990, pp. 178–188.

[5]Sarkar, S., Erlebacher, G., Hussaini, M. Y., and Kreiss, H.O., "The Analysis and Modelling of Dilatational Terms in Compressible Turbulence," *Journal of Fluid Mechanics*, Vol. 227, 1991, pp. 473–493.

[6]Morrison, J. H., Gatski, T. B., Sommer, T. P., Zhang, H. S., and So, R. M. C., "Evaluation of a Near-Wall Turbulent Closure Model in Predicting Compressible Ramp Flows," *Near-Wall Turbulent Flows*, edited by R. M. C. So, C. G. Speziale, and B. E. Launder, Elsevier, Amsterdam, 1993, pp. 239–250.

[7]Launder, B. E., Reece, G. J., and Rodi, W., "Progress in the Development of a Reynolds-Stress Turbulence Closure," *Journal of Fluid Mechanics*, Vol. 68, 1975, pp. 537–566.

[8]Speziale, C. G., Sarkar, S., and Gatski, T. B., "Modelling the Pressure-Strain Correlation of Turbulence: An Invariant Dynamical Systems Approach," *Journal of Fluid Mechanics*, Vol. 227, 1991, pp. 245–272.

[9]Fu, S., Launder, B. E., and Tselepidakis, D. P., "Accommodating the Effects of High Strain Rates in Modeling the Pressure-Strain Correlation," UMIST TR TFD/87/5, Sept. 1987.

[10]Abid, R., and Speziale, C. G., "Predicting Equilibrium States with Reynolds Stress Closures in Channel Flow and Homogeneous Shear Flow," *Physics of Fluids A*, Vol. 5, No. 7, 1993, pp. 1776–1782.

[11]Gatski, T. B., "Turbulent Flows—Model Equations and Their Solution," *Handbook of Computational Fluid Mechanics*, Academic Press, San Diego, CA, 1995 (to be published).

[12]Fernholz, H. H., Finley, P. J., Dussauge, J. P., and Smits, A. J., "A Survey of Measurements and Measuring Techniques in Rapidly Distorted Compressible Turbulent Boundary Layers," AGARDograph No. 315, 1989, pp. 12J1–12J4.

[13]Smits, A., and Muck, K.-C., "Experimental Study of Three Shock Wave/Turbulent Boundary Layer Interactions," *Journal of Fluid Mechanics*, Vol. 182, 1987, pp. 291–314.

[14]Speziale, C. G., Abid, R., and Mansour, N. N., "Evaluation of Reynolds Stress Turbulence Closures in Compressible Homogeneous Shear Flow," *ZAMP*, 1996 (to be published).

Experimental Study of Roughness Effects on the Separated Flow over a Backward-Facing Step

Byung Nam Kim* and Myung Kyoon Chung†
Korea Advanced Institute of Science and Technology, Taejon 305-701, Korea

Introduction

THE flow over a two-dimensional backward-facing step is one of the simplest reattaching turbulent shear flows, where the separation point is fixed at the step corner and the separation line is straight. There have been a large number of experimental investigations on the flow structure over a two-dimensional backward-facing step. They reveal that the turbulent flow structure and integral properties depend on 1) the initial boundary-layer state before separation, laminar or turbulent, 2) the initial boundary-layer thickness, 3) the freestream turbulence, 4) the pressure gradient, and 5) the aspect ratio (see Eaton and Johnston[1] for a review).

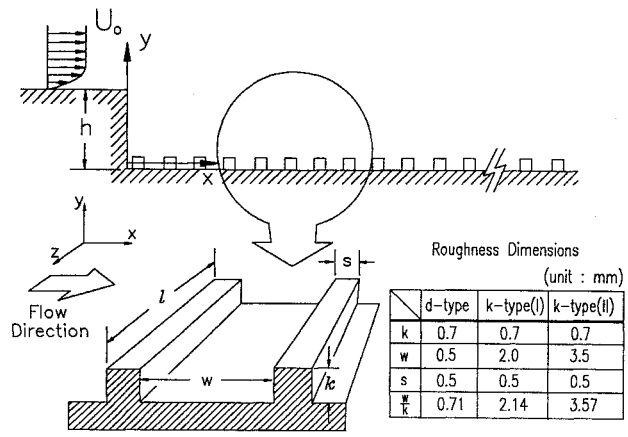

	d-type	k-type(I)	k-type(II)
k	0.7	0.7	0.7
w	0.5	2.0	3.5
s	0.5	0.5	0.5
w/k	0.71	2.14	3.57

Fig. 1 Surface roughness geometries.

In addition to these factors, since the surface roughness exerts appreciable resistance to the flow near the wall, we suspect that the surface roughness of the bottom plate may play a non-negligible role in controlling the separated recirculating and redeveloping flows. The purpose of the present study is to experimentally investigate the effects of surface roughness on the turbulent flowfield behind the step. Reattachment length, mean flowfield, fluctuating turbulent quantities, and forward flow fraction are measured by using a split film sensor.

Experimental Conditions

The experimental work was conducted in a low-turbulence level wind tunnel with a 250 × 150 mm cross section which provides a uniform flow condition at the inlet of a sudden expansion with the step height h of 20 mm. The test section and the roughness elements, which were specially designed and manufactured for the experiment, are shown schematically in Fig. 1. Conventionally when the ratio of the roughness width w to its height $k(w/k)$ is less than unity, the surface roughness is called d-type, whereas k-type roughness signifies that $w/k > 1$. In the present study, four different surface roughnesses are employed, as shown in the legend of Fig. 1. The mean velocity profile at 30 mm upstream of the step using a boundary layer pitot tube was measured. The upstream boundary-layer thickness $\delta_{0.995}$ before separation is 10.8 mm, the displacement thickness δ_* is 1.39 mm, the momentum thickness θ is 1.06 mm and the step-height Reynolds number Re_h is 26,500. Consequently, the boundary-layer shape factor H turns out to be 1.31 which is a little larger than the shape factor of 1.28 on a smooth wall.

A modified split film calibration technique of Ra et al.[2] was used to guarantee reliable calibration in a wide range of velocity magnitude and pitch angle. The experiment showed that the error in the maximum pitch angle at ±70 deg is less than 5%, and the error in the mean velocity measurement by the split film sensor is about ±2% at the maximum calibration velocity of 30 m/s. An uncertainty estimate by the Kline and McClintock method[3] showed that the error in the turbulent intensity is about 10% for its maximum value.

Experimental Results and Discussions

The velocity reversal characteristic in reattaching flows can be quantified by the forward-flow fraction. The forward-flow fraction γ_p is defined as the fraction of time for which the flow directs in the downstream direction. The reattachment point can also be determined from the distribution of the forward-flow fraction near the wall γ_{pw}. Eaton and Johnston[4] have shown that the point at which γ_{pw} is 50% coincides with the time mean reattachment point of the unsteady reattaching flow where the mean skin friction coefficient vanishes. In the present experiment, the same method reveals that the reattachment length X_R on the smooth surface is 5.86 times the step

Received June 20, 1994; revision received Sept. 12, 1994; accepted for publication Oct. 1, 1994.

*Graduate Research Assistant, Department of Mechanical Engineering,
†Professor, Department of Mechanical Engineering, Yusong-ku.